Supported Ziegler–Natta catalysts for propylene polymerization. Study of surface species formed at interaction of electron donors and TiCl$_4$ with activated MgCl$_2$

Denis V. Stukalov *, Vladimir A. Zakharov, Alexander G. Potapov, Gennady D. Bukatov

Boreskov Institute of Catalysis, Siberian Branch of the Russian Academy of Sciences, Prospect Akademika Lavrentieva 5, Novosibirsk 630090, Russia

ARTICLE INFO

ABSTRACT

Adsorption of various internal electron donors (IDs) and coadsorption of these IDs with TiCl$_4$ on activated MgCl$_2$ have been studied by DRIFT and analytical techniques. As a result, the structures of the ID species on the (104) and (110) MgCl$_2$ surfaces were proposed. Based on the v(C=O) band resolution data for the adsorbed ID, it was estimated that the activated MgCl$_2$ surface contains ca. 90% of the five-coordinated Mg cations residing on the (104) surface and ca. 10% of the four-coordinated Mg cations residing on the (110) surface. The size of ID molecule was found to influence its adsorption more significantly on the (104) MgCl$_2$ surface than on the (110) MgCl$_2$ surface. Coadsorption of the various ID and TiCl$_4$ demonstrated that TiCl$_4$ formed greatly weaker surface complexes than the ID; obviously, upon coadsorption TiCl$_4$ occupies mainly the adsorption sites that are inaccessible for the ID because of steric reasons.

1. Introduction

Heterogeneous MgCl$_2$-supported Ziegler–Natta catalysts for stereospecific olefin polymerization contain high-dispersed MgCl$_2$ as a support, TiCl$_4$ as an active component, trialkylaluminum as an activating agent, and two Lewis bases: a so-called "internal" electron donor (ID), for example ethyl benzoate (EB) or diisobutyl phthalate (DIBP), and an "external" electron donor, for example alkoxysilane [1,2]. The ID is known to play a dominant role in controlling the catalyst stereoselectivity [3–12]. Several molecular models were proposed to explain the stereoregulating capability of the ID: (i) ID blocks the (110) MgCl$_2$ surface on which aspecific active sites are likely to form [3], (ii) ID shifts the equilibrium between aspecific mononuclear Ti species and stereospecific dinuclear Ti species on the (104) MgCl$_2$ surface toward the latter species [3], (iii) ID turns aspecific Ti species into stereospecific Ti species due to coordination with Ti [4], (iv) ID turns aspecific Ti species into stereospecific Ti species due to coordination with the MgCl$_2$ surface not far from the Ti species [5–7]. However, it is not clear up to now whether one mechanism dominates over the others or some of these mechanisms have a comparable efficiency.

To understand the catalytic functioning under the molecular level, a series of contributions have been focused on studying the support structure as well as the ID and TiCl$_4$ surface species [13–30]. The modern concepts of the MgCl$_2$ surface structure, which supposedly determines the most important catalyst properties such as activity and active center heterogeneity, state that the prevailing MgCl$_2$ surfaces are (001), (104), and (110) because their surface energies calculated within periodic DFT are relatively low [17]. The basal (001) surface has no magnesium cations with chlorine vacancies, so it is of no interest to catalysis, whereas the lateral (104) and (110) surfaces involve the five- (with one chlorine vacancy) and four-coordinated (with two chlorine vacancies) Mg cations, respectively, on which the ID and TiCl$_4$ molecules may be adsorbed. The equilibrium crystal shape calculations show that the five-coordinated Mg cations are the dominant adsorption sites since the surface area of the (104) MgCl$_2$ plane is greater by several times than that of the (110) MgCl$_2$ plane [17].

Some attempts were made to estimate the distribution of the low-coordinated Mg cations from the experimental data [14,17,21,22]. To this end, the overlaps of carbonyl group vibrations in the IR spectra of ID–MgCl$_2$ samples were resolved into some components [21,22]. In Ref. [21], three components were chosen to resolve the spectra of chemisorbed EB and dibutyl phthalate, start positions of these components taken from the spectra of molecular complexes MgCl$_2$·nID. These components were attributed to the surface complexes of the ID with the five-, four-, and three-coordinated Mg cations. In Ref. [22], the spectrum of DIBP–MgCl$_2$ was an overlap of the high-frequency component,

* Corresponding author. Fax: +7 383 330 80 56.
E-mail address: stukalov@catalysis.ru (D.V. Stukalov).

which was related to physisorbed DIBP, and components of the DIBP surface complexes. To consider only the latter components, the spectrum of free DIBP was subtracted from the spectrum of DIBP–$MgCl_2$, and then the produced spectrum was resolved in two components [22]. Thus, the number of components (and their positions also) was different in the indicated papers due to the absence of evident maxima in the $v(C=O)$ bands and the overlap of components that do not relate to the chemisorbed ID, for example, the physisorbed ID and molecular complexes $MgCl_2 \cdot nID$ [21–23].

Busico et al. estimated the distribution of the low-coordinated Mg cations starting from a distinction in the amount of adsorbed $RMeSi(OMe)_2$ and $RMe_2Si(OMe)$. They supposed that $RMe_2Si(OMe)$ was chemisorbed on both the five- and four-coordinated Mg cations, while $RMeSi(OMe)_2$ was chemisorbed only on the four-coordinated Mg cations [17]. However, the formation of molecular compounds is possible here, similar to the case of the ID with carbonyl groups, and so the difference in the amounts of adsorbed alkoxysilanes can be attributed to different abilities to form the molecular complexes with $MgCl_2$.

The absence of reliable experimental data on the amount and distribution of the low-coordinated Mg cations and of the surface species formed at the interaction of ID and $TiCl_4$ with these Mg cations does not allow one to build the reliable molecular models for catalytic surface. In this connection, coadsorption of EB and $TiCl_4$ supposedly not interacting with each other directly on the $MgCl_2$ surface has recently been investigated by means of quantum chemical calculations [16]. The energetic modification upon coadsorption was found to be quite slight, and therefore the random placement of EB and $TiCl_4$ on the $MgCl_2$ surface was postulated. Nevertheless, the steric aspects of coadsorption – determining ultimately the catalyst stereoselectivity – were not considered in detail because theoretical approach cannot take into account a large enough piece of the surface.

In this work, using the diffusive reflection infrared spectroscopy (DRIFT) and analytical techniques, we investigated more thoroughly the interaction of EB and DIBP with activated $MgCl_2$ in order to find the reaction conditions in which only chemisorption of the ID takes place (the molecular compounds $MgCl_2 \cdot nID$ do not form), and finally to estimate the distribution of these IDs over the activated $MgCl_2$ surface by means of spectrum resolution for the adsorbed ID. A comparison of monoester EB and diester DIBP adsorption on the different $MgCl_2$ surfaces made it possible to suggest the structures of surface complexes of these IDs. Based on the assumed structures of surface complexes, the distribution of low-coordinated Mg cations on the activated $MgCl_2$ surface was estimated. Adsorption of the ID with different functional groups (ketones, monoesters, and diesters) and the ID differing in the size of hydrocarbon radical gave some insight into the structure of the ID surface species as well as its packing on the $MgCl_2$ surface: coordination of the monoester molecules with the $MgCl_2$ surface and steric factors regulating the ID adsorption on the (104) and (110) $MgCl_2$ surfaces were determined. The study of ID and $TiCl_4$ coadsorption in comparison with individual adsorption of the same compounds allowed us to elucidate whether $TiCl_4$ substitutes for ID on the $MgCl_2$ surface and to reveal the influence of the ID nature on $TiCl_4$ adsorption.

2. Experimental

2.1. Materials

Butylchloride, n-heptane, chlorobenzene (CB), acetonylacetone (AA), valerophenone (VP), ethyl benzoate (EB), butyl benzoate (BB), dimethyl phthalate (DMP), diisobutyl phthalate (DIBP), dioctyl phthalate (DOP), and 2,6-diacetopyridine (DAP) were used after

purification on molecular sieves. All the samples were prepared in an inert atmosphere.

2.2. Support

The activated $MgCl_2$ sample used to prepare the most $ID/MgCl_2$ and $TiCl_4/ID/MgCl_2$ samples was synthesized by the interaction of magnesium and BuCl (the molar ratio BuCl/Mg = 3) in n-heptane at 90 °C, and finally washed twice with the same solvent [31]. This $MgCl_2$ sample (S_{BET} = 108 m^2/g) contains ca. 3–5 wt.% of organic products.

The $MgCl_2$ samples particularly marked in Table 3 were prepared by dry milling of anhydrous $MgCl_2$ (5 g) in a planetary-type mill with 100 balls (diameter 3 mm) for 30 min.

2.3. Sample preparation

The $ID/MgCl_2$ samples were prepared by the interaction of ID with a suspension of activated $MgCl_2$ in CB or n-heptane at a fixed temperature for 1 h; ID was introduced after thermostating the $MgCl_2$ suspension for 10 min at a specified temperature. The products were washed twice with the indicated solvents at the same temperature. In the case of CB, the samples were extra washed with n-heptane to remove the excess of CB. Then, the samples were dried under vacuum. The details of sample synthesis (the ID loading, temperature, solvent) are presented in the tables (see below).

The $TiCl_4/ID/MgCl_2$ samples were prepared by the interaction of ID and $TiCl_4$ with a suspension of activated $MgCl_2$ in CB at 110 °C for 1 h. ID and $TiCl_4$ were loaded 30 min one after another (first ID, and then $TiCl_4$), each in the amount of 300 μmol/g of $MgCl_2$. The resulting products were washed twice with CB at 110 °C, and then twice with n-heptane at room temperature to remove the excess of CB. Then the samples were dried under vacuum.

2.4. Chemical analysis

The contents of the ID were determined by high-performance liquid chromatography using standard solutions of these compounds in acetonitrile. The content of $TiCl_4$ was determined by atomic emission spectrometry.

2.5. DRIFT measurements

DRIFT spectra were obtained on a SHIMADZU FTIR-8400S spectrometer equipped with dried nitrogen box. Samples were placed in waterproof cavities with BaF_2 windows under vacuum. Resolution of the instrument was 2 cm^{-1}.

3. Results and discussion

3.1. Influence of reaction conditions on the interaction of ID with activated $MgCl_2$

The preparation of $MgCl_2$-supported Ziegler–Natta catalysts makes a wide use of different solvents: commonly CB (a polar aromatic solvent) is needed at the stage of support interaction with ID and $TiCl_4$, while n-heptane (a nonpolar solvent) is used for catalyst washing. To study the effect of solvent on the EB interaction with activated $MgCl_2$, the reaction of EB with the chemically activated $MgCl_2$ sample was examined under the molar ratio ID/Mg = 0.1 at 30 °C. The resulting ID contents in these samples are presented in Table 1.

Experiments 1 and 2 showed that the EB interaction with the activated $MgCl_2$ was incomplete in both the solvents; however, the EB content was much higher in sample 2 than in sample 1. A

Table 1
Influence of reaction conditions on interaction between the ID and the activated MgCl$_2$.[a]

Exp. no.	ID	Solvent	T (°C)	Content of ID in sample (μmol/g MgCl$_2$)
1	EB	CB	30	260
2	-//-	n-heptane	30	410
3[b]	-//-	n-heptane	30	150
4	-//-	CB	110	184
5	DIBP	CB	30	265
6	-//-	CB	60	261
7	-//-	CB	110	180
8[c]	-//-	CB	30	230

[a] Reaction conditions: [MgCl$_2$] = 0.04 g/ml, ID/Mg = 0.1 (1000 μmol/g MgCl$_2$), 1 h.
[b] Sample 2 washed with CB at 30 °C.
[c] At first, suspension of MgCl$_2$ in CB was heated at 110 °C for 1 h, then it was cooled to 30 °C, finally DIBP was added to cooled suspension.

wide variety of products were expected to form at the interaction of Lewis bases with activated MgCl$_2$; thus, to separate the final products into some parts, the samples were washed with CB. This procedure decreased the EB content in the case of sample 2 (resulting in sample 3) and had no effect in the case of sample 1. This allows a conclusion that the reaction between EB and activated MgCl$_2$ in n-heptane, in contrast to that in CB, leads to the formation of two different groups of EB products: CB-soluble and insoluble.

The IR spectra of samples 1 and 2 in the v(C=O) region are presented in Fig. 1. The v(C=O) bands of EB in these samples were observed mainly in the region of 1640–1700 cm^{-1} and, according to the literature, were attributed to the carbonyl groups coordinated with Mg cations [32]. The v(C=O) band of EB in sample 2 is more complicated in the low-frequency region as compared to sample 1. This confirms the fact arising from the operation with the solvent sequence described above: sample 2 has a wider variety of products than sample 1. We suppose that in n-heptane EB forms both the molecular complexes MgCl$_2$·nEB, which probably dissolve in CB, and the surface complexes with the five- and four-coordinated Mg cations; whereas in CB EB forms only the surface complexes. Rigorous evidence of this assumption would be provided if one received the IR spectra with a single symmetric v(C=O) band of EB corresponding to the individual EB surface complexes, and then compared it with the spectra of samples 1 and 2. However, this is impossible because the IDs are unselective toward the nature of adsorption sites on the activated MgCl$_2$ surface, which will be demonstrated further. Nevertheless, indirect evidence of CB preventing the formation of molecular complexes consists in comparative simplicity of the spectrum of sample 1 (Fig. 1a), which can be resolved only in two components (Fig. 2)

relating to the EB complexes with the adsorption sites generally accepted.

Besides, some arguments can be drawn from the literature. The formation of new compounds MgCl$_2$·nEB denoted here as the molecular complexes is confirmed by the fact that new XRD bands for MgCl$_2$ that interacted with EB in n-heptane for some days were found in addition to the original MgCl$_2$ reflection [33,34]. Another reason is that calorimetric measurements revealed two different processes under the interaction of EB and activated MgCl$_2$ in n-heptane: a rapid first stage attributed to EB adsorption and a considerably slower second stage referred to complex formation [35].

Thus, chemisorption of the ID seems to occur in CB, whereas the less selective interaction – formation of both the surface and molecular complexes – proceeds in n-heptane. The polar solvent (CB) is likely to prohibit the formation of molecular complexes and the accompanying process of support destruction due to solvation of the activated MgCl$_2$ surface.

In order to consider the temperature effect on ID adsorption, the reactions of EB and DIBP with activated MgCl$_2$ were carried out in CB to deal only with the surface compounds. The resulting ID contents in the samples are given in Table 1. Although adsorption of EB was noticeably lower at 110 °C (sample 4) than at 30 °C (sample 1), the IR spectrum of sample 4 in the v(C=O) region was very similar to that of sample 1 (Fig. 1a), indicating that only the EB adsorption occurs at these temperatures in CB.

The reasons of temperature effect on ID adsorption were studied most thoroughly with DIBP. The amount of adsorbed DIBP was virtually equal at 30 and 60 °C (Table 1, samples 5 and 6), whereas at 110 °C it was noticeably lower (Table 1, sample 7). The former observation requires the irreversibility of DIBP adsorption, but it is in contradiction with the latter observation. To resolve this problem, the effect of heat treatment of the activated MgCl$_2$ sample was examined. At first, a suspension of MgCl$_2$ in CB was heated at 110 °C for 1 h, and then DIBP was adsorbed on this support at 30 °C (Table 1, sample 8). A decrease in the DIBP adsorption in comparison with experiment 5 can obviously be associated with the fact that the amount of adsorption sites is less at 110 than at 30 °C, which is in agreement with the literature XRD data indicating that heating of activated MgCl$_2$ diminishes its structural disordering [36]. The failure of this process at 60 °C, which is the explanation of identical DIBP adsorption at 30 and 60 °C, would be caused by the high (90 °C) temperature at which the support was synthesized.

In turn, the number of adsorption sites seems to be equal for samples 7 and 8 since both MgCl$_2$ samples were heated at
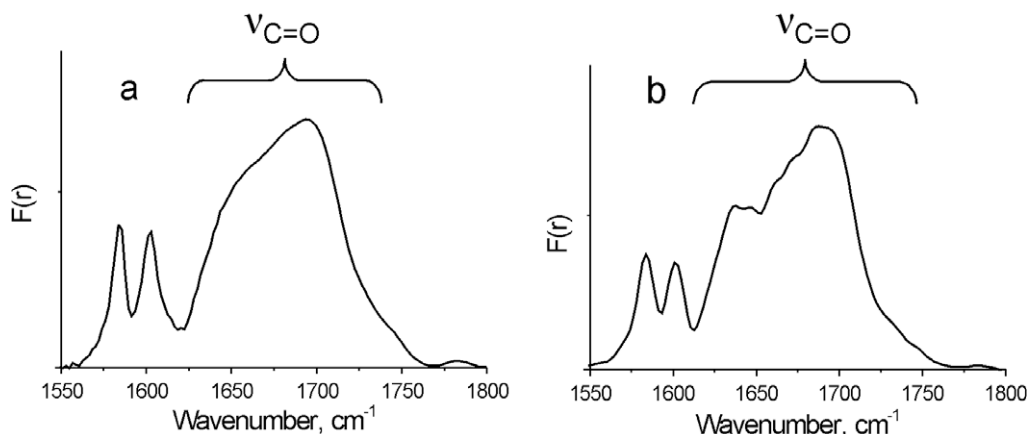

Fig. 1. The IR spectra of EB/MgCl$_2$ in the v(C=O) region obtained in CB (a) and n-heptane (b) at 30 °C (Table 1, samples 1 and 2).

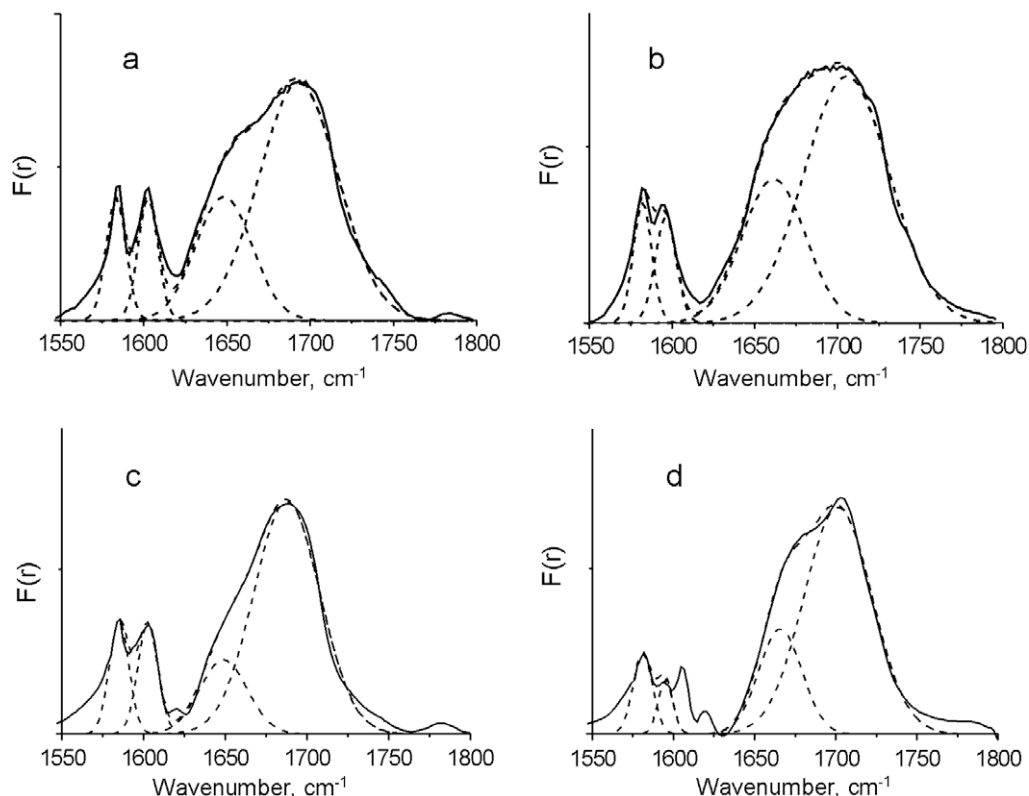**Fig. 2.** The IR spectra of EB and DIBP adsorbed on chemically activated $MgCl_2$ (a and b) and on dry-milled $MgCl_2$ (c and d) in the $v(C=O)$ region (Table 2, samples 1–4).

110 °C, but the amount of DIBP adsorbed at 110 °C (sample 7) was 20% lower than that at 30 °C (sample 8). Two explanations for this fact can be suggested: reversibility of DIBP adsorption at 110 °C or a less compact packing of DIBP on the $MgCl_2$ surface at high temperature. To verify the first hypothesis, several washings of sample 7 with CB at 110 °C were performed. These procedures did not decrease the DIBP content in the sample, thus pointing to irreversibility of DIBP adsorption at 110 °C. We therefore believe that there are two manners of DIBP packing on the $MgCl_2$ surface: a more compact packing at lower temperatures and a less compact packing at higher temperatures.

3.2. Adsorption of EB and DIBP on activated $MgCl_2$

To study the adsorption of EB and DIBP on the $MgCl_2$ surface, the interaction of these IDs with activated $MgCl_2$ was performed in CB since in that case only the adsorption of these IDs takes place (the molecular compounds do not form). First of all, adsorption iso-

therms for EB and DIBP at 110 °C were obtained. The corresponding data are presented in Table 2.

Small amounts of ID were entirely adsorbed on the support (exps. 1 and 2, 6 and 7). As soon as the limit value of adsorption is achieved, the content of these IDs becomes independent of their excess (exps. 3–5 and 8–10). Thus, the isotherm of irreversible adsorption for both EB and DIBP was observed. Strong coordination of these IDs with the surface Mg cations (adsorption heats are in the range of 20–40 kcal/mol) was also corroborated by DFT calculations [16,27]. The fact of the highest possible quantity of surface complexes in the activated $MgCl_2$ sample being equal for monoester EB and diester DIBP (184 μmol/g $MgCl_2$) is surprising, and will be explained below taking into account the DRIFT data for these samples.

The IR spectra of samples 1 and 2 (Table 3) in the $v(C=O)$ region are shown in Fig. 2. It is seen that asymmetric $v(C=O)$ bands of adsorbed EB (Fig. 2a) and DIBP (Fig. 2b) in these samples are mainly in the region of 1650–1700 cm^{-1}. As these frequencies are essentially lower than the carbonyl stretching vibrations for EB

Table 2
Adsorption of EB and DIBP on activated $MgCl_2$.[a]

Exp. no.	ID	Loading of ID (μmol/g $MgCl_2$)	Content of ID in sample (μmol/g $MgCl_2$)
1	EB	100	105
2	-//-	150	145
3	-//-	300	185
4	-//-	1000	184
5	-//-	3000	182
6	DIBP	100	103
7	-//-	150	157
8	-//-	300	182
9	-//-	1000	184
10	-//-	3000	187

  [a] Reaction conditions: CB, 110 °C, [$MgCl_2$] = 0.04 g/ml, 1 h.

Table 3
Data on the surface complexes of EB and DIBP on activated $MgCl_2$.[a]

Exp. no.	ID	Total quantity of surface complexes (μmol/g $MgCl_2$)	$v(C=O)$ for surface complexes (cm^{-1})		Quantity of surface complexes (μmol/g $MgCl_2$ (mol.%))	
			Q_4	Q_5	Q_4	Q_5
1	EB	184	1650	1692	37 (20)	147 (80)
2	DIBP	184	1662	1705	44 (24)	140 (76)
3[b]	EB	102	1649	1688	18 (18)	84 (82)
4[b]	DIBP	100	1665	1702	23 (23)	77 (77)

  [a] Reaction conditions: CB, 110 °C, [$MgCl_2$] = 0.04 g/ml, 1 h, 1000 μmol ID/g $MgCl_2$.
  [b] In these experiments, $MgCl_2$ activated by dry milling was used for EB and DIBP adsorption.

(1747 cm^{-1}) and DIBP (1752 cm^{-1}) in the gas phase, one may conclude that carbonyl groups of the adsorbed ID are coordinated with the surface Mg cations.

To determine the distribution of surface complexes, the ν(C=O) bands of the adsorbed ID were resolved in two components having a Gaussian shape. It can be seen that the ν(C=O) band of both EB and DIBP is described by two components to a high degree of accuracy (Fig. 2), so both EB and DIBP can be supposed to form predominantly two types of surface complexes. Since mainly the five- and four-coordinated Mg cations are suggested to reside on the activated MgCl$_2$ surface, it can be presumed that the lower frequencies (see Table 3) relate to stronger surface complexes $\mathbf{Q}_4$, which are formed by EB (or DIBP) and four-coordinated Mg cations on the (110) MgCl$_2$ surface, whereas the higher frequencies (see Table 3) relate to less strong surface complexes $\mathbf{Q}_5$, which are formed by EB (or DIBP) and five-coordinated Mg cations on the (104) MgCl$_2$ surface.

As a result of spectrum resolution, information about the distribution of surface complexes was obtained. Presuming that the diffusion coefficient (s) is independent of the wavelength and the molar extinction coefficient (ε) is the same for two components, in accordance with the Kubelka–Munk formula $F(R) = \varepsilon * c/s$, intensity of the component is proportional to the content of carbonyl groups. Since no components related to free carbonyl groups were revealed in the IR spectra of these samples, the absolute content of surface complexes is proportional to the amount of carbonyl groups.

The corresponding distributions of surface complexes for EB and DIBP are given in Table 3. These data indicate that the five-coordinated Mg cations significantly prevail over the four-coordinated species. The domination of the former adsorption sites was predicted by theoretical calculations indicating that the surface energy of the (104) MgCl$_2$ plane is far lower than the surface energy of the (110) MgCl$_2$ plane [17]. Another interesting point is the independence of the ID distribution from its content in the sample: the distributions of the ID surface complexes were identical for samples 1 and 4, 6 and 9 (Table 2). Thus, ID does not show any selectivity to the five- or four-coordinated Mg cations despite the fact that complexes $\mathbf{Q}_4$ are more stable than complexes $\mathbf{Q}_5$ [27].

The procedure of MgCl$_2$ activation is known to determine the features of the support structure. For example, based on the XRD data, some structure differences were found between chemically activated MgCl$_2$ and MgCl$_2$ activated by dry milling [37]. Accordingly, to elucidate the influence of the support preparation procedure on the distribution of adsorption sites, EB and DIBP were adsorbed on the MgCl$_2$ sample activated by dry milling (Table 3, samples 3 and 4).

The amounts of EB and DIBP adsorbed on dry-milled MgCl$_2$ were nearly two times lower than those adsorbed on chemically activated MgCl$_2$ (Table 3), but the distribution of surface complexes was practically the same for both activated MgCl$_2$ samples. Therefore, the distribution of adsorption sites seems to be determined only by the ratio of surface energies for free MgCl$_2$ planes. However, it could be certainly different for supports synthesized in the presence of ID, which may increase a relative proportion of less stable (110) MgCl$_2$ surface due to the change of surface energies caused by surface modification with chemisorbed ID [18]. Further, we will discuss possible molecular models for EB and DIBP adsorption on the (104) and (110) MgCl$_2$ surfaces.

Since EB and DIBP form virtually the same amount of complexes on both the (104) and (110) MgCl$_2$ surfaces (Table 3), a molecule of EB or DIBP occupies the equal number of low-coordinated Mg cations on each MgCl$_2$ surface. In view of the absence of free carbonyl groups (in accordance with the IR spectrum of adsorbed DIBP, Fig. 2b), DIBP must be coordinated by both carbonyl groups with neighboring Mg cations on the (104) surface (Fig. 3b), and so one molecule of EB occupies at least two five-coordinated Mg cations. To explain this fact, the steric difficulties (two EB molecules cannot occupy two neighboring Mg cations) or coordination of EB by both oxygen atoms with the formation of bridge complex (Fig. 3a) can be proposed.

On the (110) surface, EB can be coordinated only with one Mg cation, forming the monodentate (Fig. 3c) or chelate (Fig. 3d) complex; DIBP can be coordinated with one or two Mg cations, forming the chelate (Fig. 3e) or bridge complex (Fig. 3f). In spite of a less steric preference of DIBP molecule in comparison with EB molecule, these IDs form the equal amount of complexes on the (110) surface. A more compact chelate DIBP complex (Fig. 3e) is therefore more favorable than the bridge DIBP complex (Fig. 3f).

In accordance with the assumed structures of surface complexes, a molecule of ID (EB or DIBP) occupies at least twice more
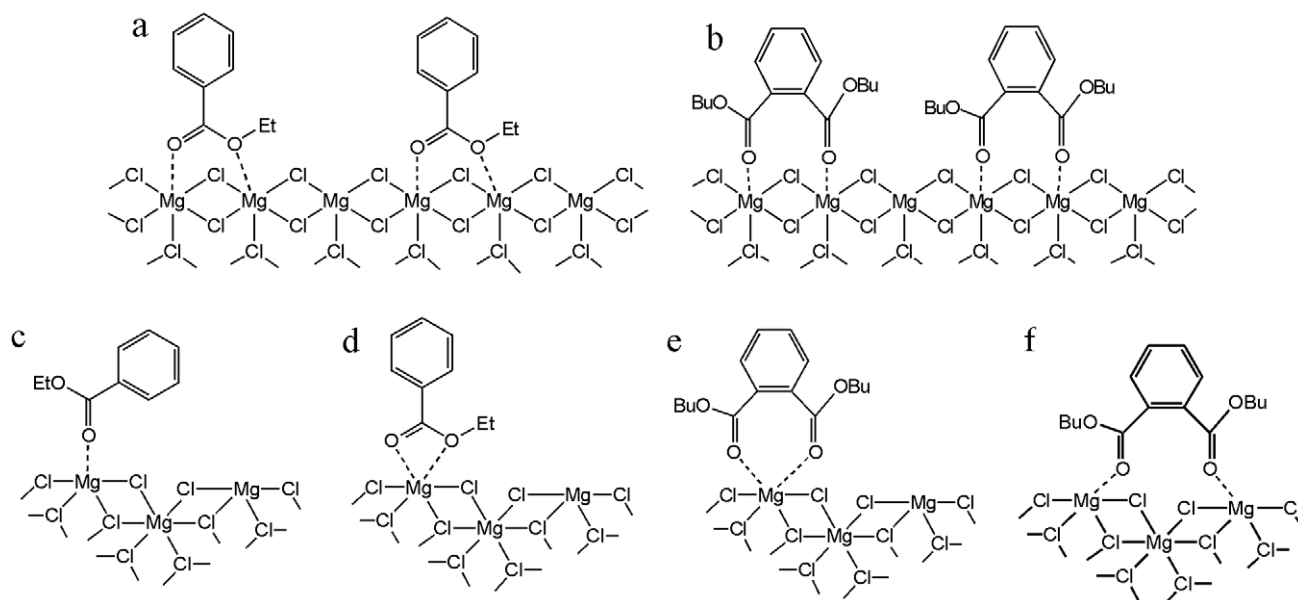

Fig. 3. Possible structures of surface complexes: EB (a) and DIBP (b) on the (104) surface; EB (c, d) and DIBP (e, f) on the (110) surface.

Mg cations on the (104) surfaces as compared to the (110) surfaces. Taking into account such stoichiometry, the distribution of low-coordinated Mg cations was estimated from the data on the fraction of Q_4 and Q_5 complexes (Table 3). The estimates show that the activated $MgCl_2$ surface contains ca. 10% of four-coordinated Mg cations and ca. 90% of five-coordinated species.

3.3. Adsorption of different IDs on activated $MgCl_2$

To clarify the structure of ID surface species and its packing on the $MgCl_2$ surface, the ID with different functional groups (ketones, monoesters, and diesters), the ID with several types of nucleophilic centers, and the ID differing in the size of hydrocarbon radical were
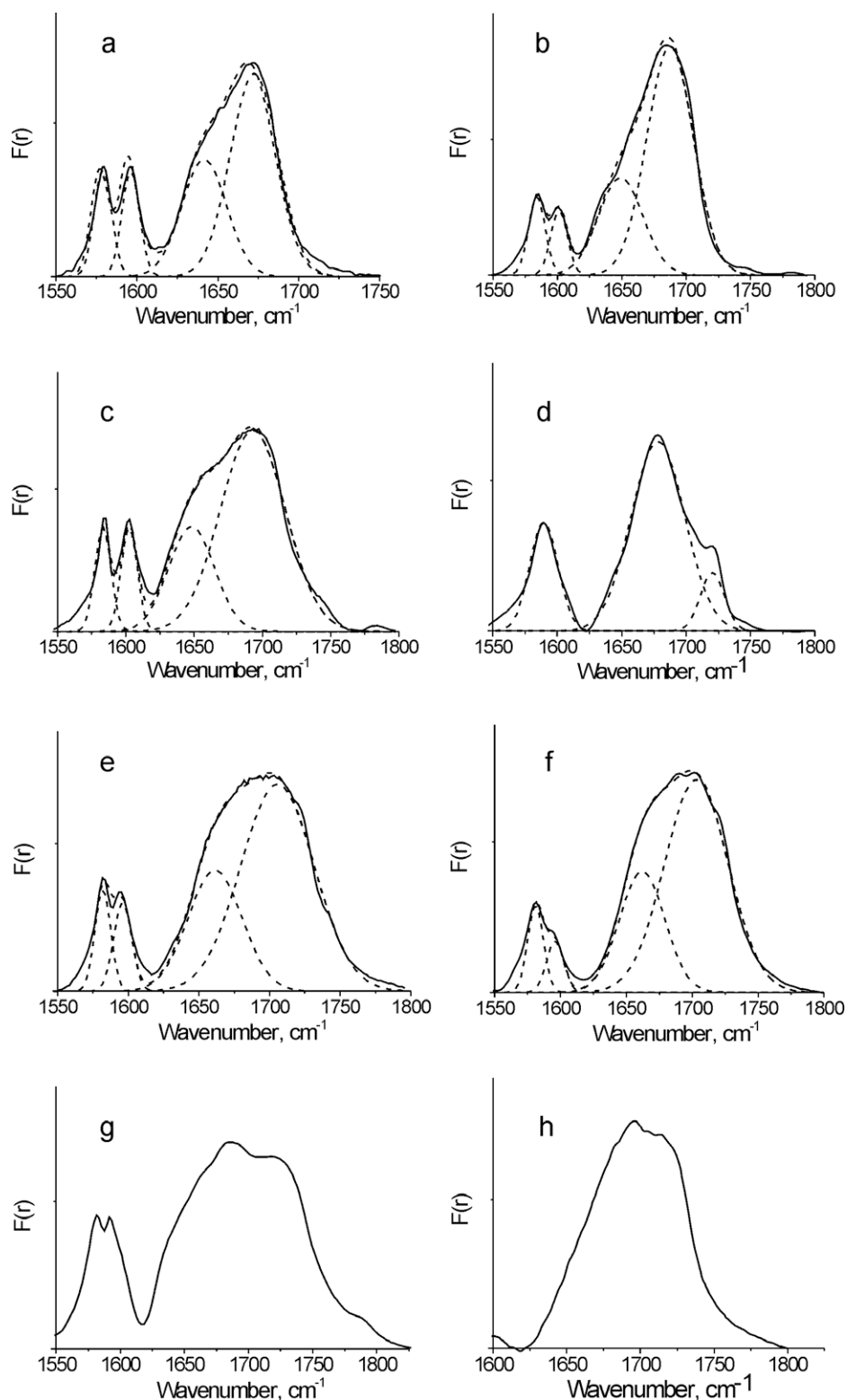

Fig. 4. The IR spectra of VP/MgCl$_2$ (a), BB/MgCl$_2$ (b), EB/MgCl$_2$ (c), DAP/MgCl$_2$ (d), DIBP/MgCl$_2$ (e), DOP/MgCl$_2$ (f), DMP/MgCl$_2$ (g), and AA/MgCl$_2$ (h) in the v(C=O) region (Table 5, samples 1–8).

employed. The interaction of these IDs with activated $MgCl_2$ was carried out in chlorobenzene at 110 °C to prevent the formation of molecular compounds $MgCl_2 \cdot nID$. To estimate the distribution of surface complexes, the $\nu(C=O)$ bands of adsorbed ID were resolved in two components as described above (the resolutions of $ID/MgCl_2$ spectra are presented in Fig. 4). The corresponding data (total content of the ID, the amounts and $\nu(C=O)$ of complexes Q_4 and Q_5) are given in Table 4.
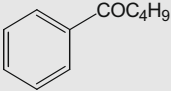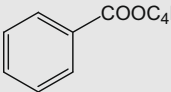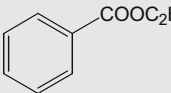
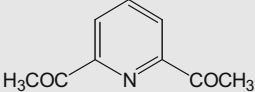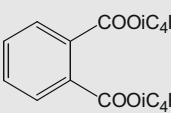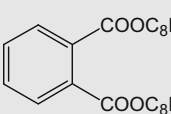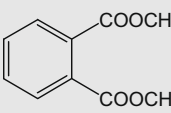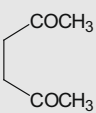### 3.3.1. Coordination of monoesters with $MgCl_2$ surface

A monoester molecule can be coordinated in two ways on each lateral $MgCl_2$ surface: monodentate by only the carbonyl oxygen and bidentate by the carbonyl and ether oxygen. The ^{13}C NMR study indicates that bidentate coordination of EB is more probable [20,25], but according to theoretical calculations bidentate conformations of EB did not make any energy minima on both $MgCl_2$ surfaces [16]. To decide between the two variants, we compared adsorption of monoester BB and ketone VP (Table 4, samples 1 and 2). Since both BB and VP were adsorbed on the same activated $MgCl_2$ sample, the number of low-coordinated Mg cations accessible for BB and VP was also the same. However, ester BB formed a 1.5 times smaller number of surface complexes than aromatic ketone VP. It means that one BB molecule occupies more low-coordinated Mg cations than one VP molecule. The molecules of VP and

BB have close sizes, that is, they are virtually identical in their steric properties; thus, we have to conclude that BB is coordinated by both oxygen atoms of the COO group. Moreover, even EB, which is more favorable for steric reasons, formed less surface complexes than VP (Table 4, samples 1 and 3).

The distributions of BB and VP on the $MgCl_2$ surface significantly differed from each other: VP formed twice more complexes Q_4 on the (110) surface and 1.5 times more complexes Q_5 on the (104) surface than BB. Thus, the BB ester seems to be coordinated by OEt and C=O functions on both the (104) $MgCl_2$ surface with the formation of bridge complex (Fig. 5a) and the (110) $MgCl_2$ surface with the formation of chelate complex (Fig. 5b). Since monodentate donor VP formed only 1.5 times more complexes on the (104) $MgCl_2$ surface than bidentate donor BB, a part of five-coordinated Mg cations residing close enough to each other on this surface is VP-free obviously because of steric difficulties between the adsorbed VP molecules. On the (110) $MgCl_2$ surface, the distance between the neighboring Mg cations is much larger, and therefore it can be supposed that VP occupies all of the four-coordinated Mg cations. Then, BB occupies only a half of them likely due to the fact that the OR group coordinated with the Mg cation screens the neighboring Mg cation for another molecule of the ester (a schematic illustration of the fact is given in Fig. 5b).

Table 4
Adsorption of different IDs on activated $MgCl_2$.[a]

Exp. no.	ID		Content of ID in sample (µmol/g $MgCl_2$)	$\nu(C=O)$ (cm^{-1})		Quantity (µmol/g $MgCl_2$ (mol.%))	
	Initialism	Structure		Q_4	Q_5	Q_4	Q_5
1	VP	(COC₄H₉ on benzene ring)	223	1642	1673	78 (35)	145 (65)
2	BB	(COOC₄H₉ on benzene ring)	145	1650	1692	44 (30)	101 (70)
3	EB	(COOC₂H₅ on benzene ring)	184	1650	1692	37 (20)	147 (80)
4	DAP	(H_3COC—pyridine—$COCH_3$)	110	1720	1678	13 (12)	97 (88)
5	DIBP	(COOiC₄H₉, COOiC₄H₉ on benzene)	184	1662	1705	44 (24)	140 (76)
6	DOP	(COOC₈H₁₇, COOC₈H₁₇ on benzene)	146	1662	1705	42 (29)	104 (71)
7	DMP	(COOCH₃, COOCH₃ on benzene)	720	–	–	–	–
8	AA	(COCH₃, COCH₃ chain)	740	–	–	–	–

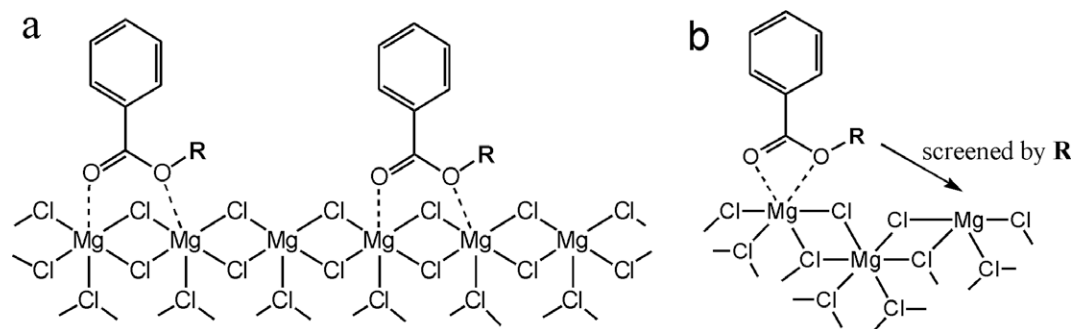[a] Reaction conditions: CB, 110 °C, $[MgCl_2]$ = 0.04 g/ml, 1 h, 1000 µmol ID/g $MgCl_2$.

Fig. 5. Possible monoester (EB, BB) complexes: on the (104) surface (a) and on the (110) surface (b).

3.3.2. Coordination of DAP with MgCl$_2$ surface

To understand the significance of the nature of nucleophilic center for ID coordination with the MgCl$_2$ surface, adsorption of DAP (Table 4, sample 4) having several nucleophilic centers (one nitrogen and two oxygen atoms) was studied. The v(C=O) band of adsorbed DAP was an overlap of the component at 1678 cm^{-1} with high intensity and of the component at 1720 cm^{-1} with low intensity (Fig. 4d). The v(C=O) band of free DAP dissolved in heptane was at ca. 1710 cm^{-1}. Since coordination of carbonyl groups with low-coordinated Mg cations results in a decrease of v(C=O), only the component at 1678 cm^{-1} relates to carbonyl groups coordinated with the MgCl$_2$ surface. The shift of this component, $\Delta v = 32$ cm^{-1}, was identical to the shift of component related to DIBP complexes on the (104) MgCl$_2$ surface, and so the component at 1678 cm^{-1} can be supposed to correspond to the DAP complexes on the (104) MgCl$_2$ surface. In contrast to the spectra of ketone and monoesters adsorbed on activated MgCl$_2$ (Fig. 4a–c), there was no low-frequency component in the spectrum of adsorbed DAP (Fig. 4d). Therefore, DAP seems to be coordinated only by the nitrogen (without carbonyl groups) on the (110) surface since the distance between neighboring Mg cations is large enough for carbonyl groups to be also coordinated. The component at 1720 cm^{-1} obviously corresponds to free carbonyl groups of DAP coordinated only by the nitrogen on the (110) surface.

It should be noted that the v(C=O) bands of the most adsorbed ID (ketones, monoesters, and diesters) have no distinct maxima, and resolution of these bands was carried out on the assumption that two types of adsorption sites (the four- and five-coordinated Mg cations) dominate on the activated MgCl$_2$ surface. In turn, adsorption of DAP clearly confirms this assumption since there are only two distinct components in the v(C=O) band of adsorbed DAP.

3.3.3. Steric aspects of ID adsorption on MgCl$_2$ surface

Since ID molecules are large enough, it could be expected that a part of adsorption sites on the MgCl$_2$ surface is inaccessible to ID because of steric difficulties. To determine the significance of steric factor, adsorption of the ID differing in the size of hydrocarbon radical was compared.

In the group comprising both monoesters and diesters, the following regularity was observed: the larger is the ID hydrocarbon radical, the lower is the number of complexes formed by ID on the MgCl$_2$ surface (Table 4, samples 2 and 3, 5 and 6). It can be seen from the distributions of EB and BB (or DIBP and DOP) that adsorption of ID with a larger hydrocarbon radical was low only on the (104) surface; the contents of EB and BB (or DIBP and DOP) were close enough to each other on the (110) surface and differed ca. 1.5 times on the (104) surface. This fact demonstrates that the steric difficulties are far stronger on the (104) surface than on the (110) surface obviously because in the first case the distance be-

tween neighboring Mg cations is 1.7 times less than that in the second case.

The special situations were observed for DMP and AA. The contents of these IDs (Table 4, samples 7 and 8) were several times higher than the content of DIBP, which forms only the surface complexes under interaction with activated MgCl$_2$ in CB. Moreover, the v(C=O) bands of DMP/MgCl$_2$ and AA/MgCl$_2$ (Fig. 4g and h), in contrast to most ID (Fig. 4a–f), were significantly broadened due to components with frequencies higher than 1710 cm^{-1}, which may correspond to molecular complexes MgCl$_2$·nID [32]. These facts allow us to conclude that the IDs with methyl radicals screening quite poorly the carbonyl groups (DMP and AA) are more active than the IDs with hydrocarbon radicals efficiently screening the carbonyl groups: formation of both the surface complexes and the molecular compounds was observed for such ID even in CB.

3.4. Coadsorption of TiCl$_4$ and ID on MgCl$_2$ surface

Firstly, we examined adsorption of TiCl$_4$ in the absence of ID. To determine the highest possible quantity of TiCl$_4$ surface complexes, the activated MgCl$_2$ sample was treated by different amounts of TiCl$_4$ in CB at 110 °C (the resulting samples were washed twice with CB at the same temperature). The corresponding data are given in Table 5. A small amount of TiCl$_4$ was entirely adsorbed on the support (Table 5, exp. 1). As soon as the limit value of adsorption (120 μmol/g MgCl$_2$) is achieved, the content of TiCl$_4$ in the sample becomes independent of its excess (Table 5, exps. 2 and 3), thus pointing to irreversibility of TiCl$_4$ adsorption. A comparison of the TiCl$_4$ adsorption value with that of ID adsorption can allow us to elucidate the ability of TiCl$_4$ to be adsorbed on different MgCl$_2$ surfaces. Since for most ID (see Table 4) the quantity of ID complexes on the (110) MgCl$_2$ surface was ca. 40 μmol/g MgCl$_2$, it can be concluded that TiCl$_4$ forms complexes on the (104) MgCl$_2$ surface anyhow. On account of a larger unsaturation of Mg cations on the (110) MgCl$_2$ surface compared to the (104) MgCl$_2$ surface, it should be expected that TiCl$_4$ forms complexes on the (110) MgCl$_2$ surface too.

Further, we investigated coadsorption of ID and TiCl$_4$ under their equal loadings (300 μmol/g MgCl$_2$); first, the ID was loaded, and then TiCl$_4$. To study the influence of the ID nature on TiCl$_4$

Table 5
Adsorption of TiCl$_4$ on activated MgCl$_2$.[a]

Exp. no.	Loading of TiCl$_4$ (μmol/g MgCl$_2$)	Content of TiCl$_4$ in sample (μmol/g MgCl$_2$)
1	100	95
2	1000	117
3	10,000	120

[a] Reaction conditions: CB, 110 °C, [MgCl$_2$] = 0.04 g/ml, 1 h.

Table 6
Coadsorption of ID and TiCl$_4$ on activated MgCl$_2$.

Exp. no.	ID	Content in sample (µmol/g MgCl$_2$)	
		ID	TiCl$_4$
1	–	–	120
2	VP	220	88
3	EB	162	108
4[a]	-//-	170	93
5	BB	145	90
6	DIBP	171	72
7	DOP	126	40
8[a]	-//-	120	65
9	DMP	282	148
10	AA	300	200

[a] In these exps. adsorption order was firstly TiCl$_4$ then the ID.

adsorption, a number of TiCl$_4$/ID/MgCl$_2$ samples with ID from Table 4 were obtained. The content of ID and TiCl$_4$ in these samples is presented in Table 6. The content of ID in samples 2, 3, 5, 6, and 7 (Table 6) was close to its content in samples 1, 2, 3, 5, and 6 (Table 4) obtained without TiCl$_4$. Moreover, the ν(C=O) bands of the adsorbed ID were virtually identical both in the presence and in the absence of TiCl$_4$. As an illustration, the IR spectra of

samples containing EB and DOP in the ν(C=O) region are presented in Fig. 6.

Coadsorption of ID and TiCl$_4$ is seen to be virtually noncompetitive: TiCl$_4$ can substitute only a small portion of ID on the MgCl$_2$ surface (Table 6, exps. 2, 3, 5, 6, and 7), whereas ID can substitute a significant portion of TiCl$_4$ on the MgCl$_2$ surface (Table 6, exps. 4 and 8). It means that TiCl$_4$ forms less strong complexes on the MgCl$_2$ surface than ID, and must occupy mostly the adsorption sites that are inaccessible to ID because of steric difficulties created by adsorbed ID molecules. As an illustration, Fig. 7 shows the possible structure of coadsorption site on the (1 0 4) MgCl$_2$ surface, including dibutyl phthalate (DBP) and TiCl$_4$ adsorbed on the coupled five-coordinated Mg cations, which are inaccessible to DBP molecules due to steric difficulties. This can be given the sense of adsorbed DBP molecules forming the "cages" for TiCl$_4$ species on the MgCl$_2$ surface.

Thus, coadsorption of ID and TiCl$_4$ can be presented in the following way. At first, ID occupies all the accessible Mg cations, forming a tight covering on the MgCl$_2$ surface, which plays the role of a special matrix for TiCl$_4$, after that TiCl$_4$ occupies the rest ID-free adsorption sites. This coadsorption scheme meets the requirements of the earlier proposed mechanism for stereoregulation by ID, according to which the ID, being in close proximity to the Ti
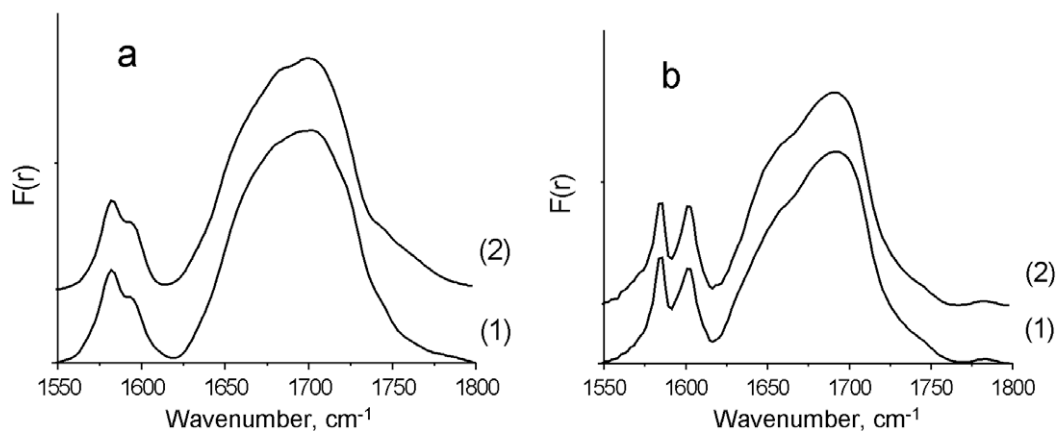

Fig. 6. The IR spectra: DOP/MgCl$_2$ (1a), DOP/TiCl$_4$/MgCl$_2$ (2a); EB/MgCl$_2$ (1b), EB/TiCl$_4$/MgCl$_2$ (2b) in the ν(C=O) region (Table 5, samples 3 and 6; Table 7, samples 3 and 7).
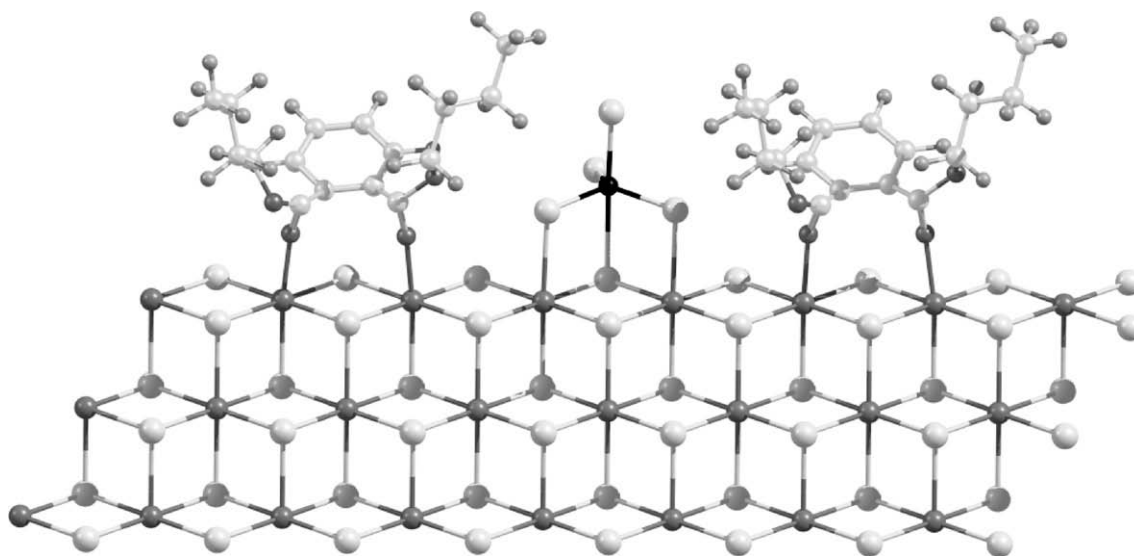

Fig. 7. A possible scheme of DBP and TiCl$_4$ coadsorption on the (1 0 4) MgCl$_2$ surface.

species, creates the so-called bulkiness for monomer molecule to be oriented at the active center in a certain way [5–7]. Considering the entire catalytic surface, it is clear that the ID covering, being a matrix for $TiCl_4$, regulates the $TiCl_4$ location on the $MgCl_2$ surface.

Since the ID covering is a matrix for $TiCl_4$ on the $MgCl_2$ surface, the ID nature should be expected to affect the $TiCl_4$ adsorption. Coadsorption with VP, EB, BB, DIBP, and DOP decreased the $TiCl_4$ content in the sample to a different degree, indicating that IDs differ in their ability to block the $MgCl_2$ surface for $TiCl_4$. Diesters (DIBP and DOP) block the $MgCl_2$ surface more efficiently than monoesters (EB and BB). In addition, a common regularity was observed in each of these groups: the larger is the ID hydrocarbon radical, the lower is the amount of $TiCl_4$ adsorbed on the $MgCl_2$ surface (Table 6, samples 3 and 5, 6 and 7, respectively). It is evident that hydrocarbon radical of the adsorbed ID takes part in blocking of the $MgCl_2$ surface for $TiCl_4$. To understand the nature of this effect, we tested the influence of the adsorption order.

To this end, adsorption of the ID (EB and DOP) and $TiCl_4$ was carried out in the reverse order: first $TiCl_4$, and then the ID (Table 6, samples 4 and 8). In the case of EB, only a minor influence of adsorption order was observed: the contents of EB and $TiCl_4$ in samples 3 and 4 were close to each other. In the case of DOP, adsorption of $TiCl_4$ before DOP provided a 1.6-fold increase in the $TiCl_4$ content in comparison with the reverse adsorption order (Table 6, samples 7 and 8). This indicates that a part of low-coordinated Mg cations in sample 7 is not accessible to $TiCl_4$ because of kinetic difficulties produced by hydrocarbon radicals of the adsorbed DOP. In this connection, a part of Ti species in the catalyst containing the ID with a large hydrocarbon radical is expected to be inactive in polymerization due to kinetic screening of the $MgCl_2$ surface.

Special situations were observed in experiments 9 and 10 (Table 6) in which the ID interacted with activated $MgCl_2$ entirely. In these samples, the content of $TiCl_4$ was significantly higher than that in sample 1 (Table 6). As shown above, the interaction of AA and DMP with activated $MgCl_2$ (Table 4, samples 7 and 8) results in the formation of molecular complexes $MgCl_2 \cdot nID$; so, we suppose that the additional amount of $TiCl_4$ in samples 9 and 10 (Table 6) can be associated with the formation of $TiCl_4 \cdot nID$ complexes, which form as a result of interaction between molecular complexes $MgCl_2 \cdot nID$ and $TiCl_4$.

4. Conclusions

The study of the influence of reaction conditions on the interaction of EB and DIBP with activated $MgCl_2$ showed that the type of solvent strongly affects the selectivity of the interaction. Only the chemisorption of the ID occurs in CB (polar solvent), whereas a less selective interaction – formation of both the surface complexes and molecular complexes $MgCl_2 \cdot nID$ – takes place in n-heptane (nonpolar solvent). A pronounced effect of temperature on adsorption of the ID was observed. At high temperatures, the ID adsorption was lower due to a decrease in the quantity of low-coordinated Mg cations and a less compact packing of the ID on the $MgCl_2$ surface.

The samples in which EB and DIBP were only in chemisorbed state were studied by DRIFT. The $v(C=O)$ band of both EB and DIBP was described by two components to a high degree of accuracy. It was presumed that the lower frequencies relate to stronger surface complexes Q_4, which are formed by EB (or DIBP) and four-coordinated Mg cations, whereas the higher frequencies relate to less strong surface complexes Q_5, which are formed by EB (or DIBP) and five-coordinated Mg cations. In accordance with the assumed structures of surface complexes, the distribution of low-coordinated Mg cations on the activated $MgCl_2$ surface was estimated.

The activated $MgCl_2$ surface contains ca. 90% of five-coordinated Mg cations residing on the (104) surface and ca. 10% of four-coordinated Mg cations residing on the (110) surface.

The study of adsorption of the ID with different chemical structures on activated $MgCl_2$ revealed that:

(i) the monoesters are coordinated by both oxygen atoms with the $MgCl_2$ surface;
(ii) the role of steric factor is more significant on the (104) $MgCl_2$ surface than on the (110) $MgCl_2$ surface: the larger is the ID hydrocarbon radical, the smaller is the number of complexes formed by ID on the (104) $MgCl_2$ surface;
(iii) the IDs with methyl as a hydrocarbon radical are more active than other IDs: the formation of both the surface complexes and the molecular compounds takes place;
(iv) adsorption of DAP (the ID with several types of nucleophilic centers) obviously confirms that there are only two types of adsorption sites on the activated $MgCl_2$ surface.

The study of $TiCl_4$ and ID coadsorption on the activated $MgCl_2$ sample and comparison of these data with adsorption of individual compounds allow us to formulate the following coadsorption principles:

(i) coadsorption of the ID and $TiCl_4$ is noncompetitive: $TiCl_4$ forms much weaker complexes than the ID on the $MgCl_2$ surface;
(ii) the ID forms a special matrix for $TiCl_4$ on the $MgCl_2$ surface: $TiCl_4$ occupies the adsorption sites that are inaccessible to the ID for steric reasons;
(iii) the $TiCl_4$ surface species are located in the tight environment of the ID surface species;
(iv) the ID blocks the $MgCl_2$ surface for $TiCl_4$ due to coordination with the surface Mg cations and screening of the nearest adsorption sites by hydrocarbon radicals of the adsorbed ID.

References

[1] P.G. Barbe, G. Ceccin, L. Noristi, Adv. Polym. Sci. 81 (1981) 1.
[2] E.P. Moore Jr., Polypropylene Handbook: Polymerization, Hanser Publishers, New-York, 1996.
[3] V. Busico, P. Corradini, L. Martino, A. Proto, V. Savino, Makromol. Chem. 186 (1985) 1279.
[4] K. Soga, T. Shiono, Y. Doi, Makromol. Chem. 189 (1988) 1531.
[5] B. Liu, T. Nitta, H. Nakatani, M. Terano, Macromol. Chem. Phys. 204 (2003) 395.
[6] V. Busico, R. Cipullo, G. Monaco, G. Talarico, M. Vacatello, J.C. Chadwick, A.L. Segre, O. Sudmeijer, Macromolecules 32 (1999) 4173.
[7] A. Correa, F. Piemontesi, G. Morini, L. Cavallo, Macromolecules 40 (2007) 9181.
[8] V. Busico, P. Corradini, A. Ferraro, A. Proto, Makromol. Chem. 187 (1986) 1125.
[9] M.C. Sacchi, F. Forlini, I. Tritto, R. Mendichi, G. Zannoni, Macromolecules 25 (1992) 5914.
[10] J.C. Chadwick, G. Morini, G. Balbontin, I. Camurati, J.J.R. Heere, I. Mingozzi, F. Testoni, Macromol. Chem. Phys. 202 (2001) 1995.
[11] G.D. Bukatov, V.A. Zakharov, Macromol. Chem. Phys. 202 (2001) 2003.
[12] B. Liu, R. Cheng, Z. Liu, P. Qiu, S. Zhang, T. Taniike, M. Terano, K. Tashino, T. Fujita, Macromol. Symp. 260 (2007) 42.
[13] U. Giannini, Makromol. Chem. Suppl. 5 (1981) 216.
[14] V.A. Zakharov, E.A. Paukshtis, T.B. Mikenas, A.M. Volodin, E.N. Vitus, A.G. Potapov, Macromol. Symp. 89 (1995) 55.
[15] D.A. Trubitsyn, V.A. Zakharov, I.I. Zakharov, J. Mol. Catal. A: Chem. 270 (2007) 164.
[16] T. Taniike, M. Terano, Macromol. Rapid Commun. 28 (2007) 1918.
[17] V. Busico, M. Causa, R. Cipullo, R. Credendino, F. Cutillo, N. Friederichs, R. Lamanna, A. Segre, V. Castelli, J. Phys. Chem. C 112 (2008) 1081.
[18] A. Andoni, J.C. Chadwick, J.W. Niemantsverdriet, P. Thune, J. Catal. 257 (2008) 81.
[19] E. Albizzati, M. Galimberti, U. Giannini, G. Morini, Macromol. Symp. 48/49 (1991) 223.
[20] P. Sormunen, T. Hjertberg, E. Iiskola, Macromol. Chem. 191 (1990) 2663.
[21] A.G. Potapov, G.D. Bukatov, V.A. Zakharov, J. Mol. Catal. A: Chem. 246 (2006) 248.
[22] Y.V. Kissin, X. Liu, D.J. Pollick, N.L. Brungard, M. Chang, J. Mol. Catal. A: Chem. 287 (2008) 44.

[23] W. Sony, K. Chu, H. Chang, S. Ihm, J. Mol. Catal. 84 (1993) 109.
[24] H. Mori, K. Hasebe, M. Terano, J. Mol. Catal. A: Chem. 140 (1999) 165.
[25] J.C.W. Chien, L.C. Dickinson, J. Vizzini, J. Polym. Sci. A 28 (1990) 2321.
[26] A.G. Potapov, V.V. Kriventsov, D.I. Kochubey, G.D. Bukatov, V.A. Zakharov, Macromol. Chem. Phys. 198 (1997) 3477.
[27] A. Correa, G. Talarico, G. Morini, L. Cavallo, in: M. Terano (Ed.), Current Achievements on Heterogeneous Olefin Polymerization Catalysts, Sankeisha Co. Ltd., Nagoya, 2004, p. 44.
[28] L. Brambilla, G. Zerbi, F. Piemontesi, S. Nascetti, G. Morini, J. Mol. Catal. A: Chem. 263 (2007) 103.
[29] G. Monaco, M. Toto, G. Guerra, P. Corradini, L. Cavallo, Macromolecules 33 (2000) 8953.
[30] T. Taniike, M. Terano, Macromol. Rapid Commun. 29 (2008) 1472.

[31] USSR Patent 726702 (1978), V.A. Zakharov, S.I. Makhtarulin (invs.), Chem. Abstr. 95, 1981. 220579x.
[32] M. Ystenes, Ø. Bache, O.M. Bade, R. Blom, J.L. Eilertsen, Ø. Nirisen, M. Ott, K. Svendsen, E. Rytter, in: M. Terano, T. Shiono (Eds.), Future Technology for Polyolefin and Olefin Polymerization Catalysis, Technology and Education Publishers, Tokyo, 2002, p. 184.
[33] B. Keszler, G. Bodor, A. Simon, Polymer 21 (1980) 1037.
[34] S. Sergeev, G. Bukatov, V. Zakharov, E. Moroz, Makromol. Chem. 184 (1983) 2421.
[35] B. Keszler, A. Gröbler, E. Takács, A. Simon, Polymer 22 (1981) 818.
[36] Yu.I. Yermakov, B.N. Kuznetsov, V.A. Zakharov, Catalysis by Supported Complexes, Elsevier, Amsterdam, 1981, p. 214.
[37] V.A. Zakharov, D.V. Perkovets, G.D. Bukatov, S.A. Sergeev, E.M. Moroz, S.I. Makhtarulin, Kinet. Catal. 29 (1988) 903.